## Measuring equality horizon with the zero-crossing of the galaxy correlation function

F. Prada<sup>1</sup>, A. Klypin<sup>2</sup>, G. Yepes<sup>3</sup>, S. E. Nuza<sup>4</sup>, S. Gottlöber<sup>4</sup>

<sup>1</sup>Instituto de Astrofísica de Andalucía (CSIC), E-18080 Granada, Spain

<sup>2</sup>Astronomy Department, New Mexico State University, Las Cruces NM, USA

<sup>3</sup>Departamento de Física Teórica, Universidad Autónoma de Madrid, Spain

<sup>4</sup>Leibniz-Institut für Astrophysik Potsdam (AIP), Germany

(Dated: October 30, 2018)

The size of the horizon at the matter-radiation equality is a key scale of the Big Bang cosmology that is directly related to the energy-matter content of the Universe. In this letter, we argue that this scale can be accurately measured from the observed clustering of galaxies in new large scale surveys. We demonstrate that the zero-crossing,  $r_c$ , of the 2-point galaxy correlation function is closely related to the horizon size at matter-radiation equality for a large variety of flat  $\Lambda$ CDM models. Using large-volume cosmological simulations, we also show that the pristine zero-crossing is unaltered by non-linear evolution of density fluctuations, redshift distortions and galaxy biases. This makes  $r_c$  a very powerful standard ruler that can be accurately measured, at a percent level, in upcoming experiments that will collect redshifts of millions of galaxies and quasars.

PACS numbers: 98.80.-k, 98.80.Es, 98.65.Dx

The science exploitation of upcoming experiments such as BOSS, DES, LSST, BigBOSS and Euclid that will survey the uncharted universe taking spectra and images of millions of galaxies and quasars, combined with the analysis of Grand Challenge cosmological simulations and development of theoretical models, will be critical to accurately measure the properties of our Universe (e.g. [1] for a review).

The physics governing the evolution of perturbations in CDM universes imprints two distinct length scales in the galaxy distribution which are useful as "standard rulers" for distance estimates: (1) the scale of the particle horizon at matter-radiation equality and (2) the sound horizon scale at the baryon-drag epoch before recombination [2, 3]. The Baryonic Acoustic Oscillations (BAO), related with the later, have been detected in the SDSS, 2dFGRS and WiggleZ galaxy power spectra at a characteristic scale  $k_{\text{bao}} > 0.05 \, h\text{Mpc}^{-1}$ , and as a single peak in the galaxy two-point correlation function (CF) at  $r_{\text{bao}} \approx 105 \, h^{-1}\text{Mpc}$  (e.g. [4–8]).

The total physical matter density ( $\omega_{\rm m} \equiv \Omega_{\rm m} h^2 = \Omega_{\rm cdm} h^2 + \Omega_{\rm b} h^2$ ) and, thus, the moment of equality can be measured from CMB fluctuations alone, but the measurement errors decline almost by a factor of two if BAO clustering estimates are included [9]. It would be helpful to have another method for testing the equality epoch, which is more sensitive to  $\omega_{\rm m}$  than BAO.

The particle horizon at matter-radiation equality is associated with the most prominent feature of the linear power spectrum of density fluctuations P(k) - the turnover or maximum - at the characteristic scale  $k_{\rm max} \sim 0.015 \, h{\rm Mpc}^{-1}$ . This corresponds to the transition from  $P(k) \sim k$  for a Harrison-Zeldovich scale-invariant spectrum to a  $P(k) \sim k^{-3}$  spectrum due to modes that were not growing after they entered the horizon during the radiation dominated era [10]. Thus, we expect that the location of this turnover will be related to the scale of the horizon at matter-radiation equality  $k_{\rm eq}$  [3].

The equality wavenumber  $k_{\rm eq}$  is given by  $k_{\rm eq} = a_{\rm eq} H_{\rm eq}(a_{\rm eq})$  with  $a_{\rm eq} = (\omega_\gamma/\omega_{\rm m})(1+0.2271N_{\rm eff})$  and  $H_{\rm eq}(a_{\rm eq}) = \sqrt{2\Omega_{\rm m}}H_0(1/a_{\rm eq})^{3/2}$  being the scale factor and expansion rate at matter-radiation equality [2]. We adopt a radiation density  $\omega_\gamma \equiv \Omega_\gamma h^2 = 2.469 \times 10^{-5}$  and  $N_{\rm eff} = 3.04$  for standard neutrino species [9]. Hence, it can be seen that the equality horizon scale depends solely on the matter density as  $k_{\rm eq} \propto \omega_{\rm m}$ . The size of the horizon at the matter-radiation equality epoch is defined by the comoving distance  $r_{\rm eq} \equiv D_{\rm H} = \int_0^{a_{\rm eq}} [a^{-2}/H(a)] da = (4-2\sqrt{2}) k_{\rm eq}^{-1}$ . Thus,  $r_{\rm eq}$  scales with matter density as  $r_{\rm eq} \propto \omega_{\rm m}^{-1}$ . We obtain  $k_{\rm eq} \simeq 0.014 \, h{\rm Mpc}^{-1}$  and  $r_{\rm eq} \simeq 85 \, h^{-1}{\rm Mpc}$  adopting the latest matter density observational constraints [9].

The turnover in P(k) shifts to high wavenumbers for models with larger matter density mainly as a result of the scaling relation between the equality wavenumber  $k_{\rm eq}$ and  $\omega_{\rm m}$ . The matter perturbations remain frozen after entering the horizon, but since this process is not instantaneous the transition from the  $P(k) \propto k$  to  $P(k) \propto k^{-3}$ is broad over about an order of magnitude in k. For dark matter-baryonic models the expected scaling with matter density might involve an additional dependence on other cosmological parameters. In order to derive a relation between  $k_{\text{max}}$  at the maximum of P(k) and the equality scale  $k_{\rm eq}$ , we computed the linear matter power spectrum of density fluctuations of a flat ΛCDM universe, using CAMB [11], for a number of cosmological models with varying  $\omega_{\rm m}$  and  $\omega_{\rm b}$  around our fiducial model. For this fiducial model, which is consistent with WMAP7 cosmological parameters and other recent cosmological constraints ([9] and references therein), we assume the matter density  $\omega_{\rm m} = 0.132$ , the normalization of fluctuations  $\sigma_8 = 0.82$ , the primordial index of scalar perturbations  $n_{\rm s}=0.95,$  the baryon density  $\omega_{\rm b}=0.023,$  the Hubble constant  $H_0 = 100 h \,\mathrm{km} \,\mathrm{s}^{-1} \mathrm{Mpc}^{-1}$  with h = 0.7, and  $N_{\rm eff} = 3.04$ . In Fig. 1 (top panel), we show the linear matter power spectrum of our ACDM models, com-

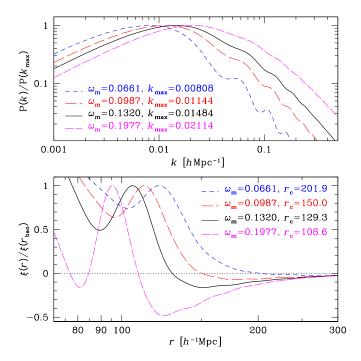


FIG. 1. Linear power spectra P(k) (top panel), and their corresponding correlation functions  $\xi(r)$  (bottom panel) for  $\Lambda$ CDM models with a fixed baryon density  $\omega_{\rm b}=0.023$ . Thick lines corresponds to our fiducial model. When  $\omega_{\rm m}$  increases, the turnover in P(k) and its characteristic scale  $k_{\rm max}$  moves to larger k. Thus, the zero-crossing in the correlation function  $\xi(r_{\rm c})=0$ , located beyond the BAO peak, shifts to smaller radii. For each model, both P(k) and  $\xi(r)$  have been normalized to its maximum and BAO peak respectively.

puted with CAMB, for different  $\omega_{\rm m}$  values and kept fixed the other cosmological parameters that determine P(k), to that given by our fiducial model. As expected, the turnover location  $k_{\rm max}$  is close to  $k_{\rm eq}$  and scales with  $\omega_{\rm m}$ . Yet, the precise turnover scale  $k_{\rm max}$  depends slightly on other cosmological parameters such as the primordial tilt  $n_{\rm s}$ .

We show in Fig. 2 (left panel) the dependence of  $k_{\rm max}$  as a function of the expected equality wavenumber  $k_{\rm eq}$  for different models with fixed baryon density 25% below and above that of our fiducial model with  $\omega_{\rm b}=0.023$  (solid line), i.e.  $\sim 6\sigma$  around best observational constraints. Matter density  $\omega_{\rm m}$  varies over a large range from 0.05 to 0.25 around our fiducial value  $\omega_{\rm m}=0.132$  (solid symbol). We kept fixed  $\sigma_8$  and  $n_{\rm s}$ . The dotted line represents the  $k_{\rm max}\equiv k_{\rm eq}$  relation which scales only with  $\omega_{\rm m}$  as  $k_{\rm eq}=0.104\,\omega_{\rm m}\,h{\rm Mpc}^{-1}$ . The difference between  $k_{\rm max}$  and  $k_{\rm eq}$  is less than 20% for the range of parameters considered here. Models with smaller baryon content show a better agreement between  $k_{\rm max}$  and  $k_{\rm eq}$ . The weak dependence of  $k_{\rm max}(k_{\rm eq})$  on baryon density  $\omega_{\rm b}$  can be approximated by

$$k_{\text{max}} = \left(\frac{0.194}{\omega_{\text{b}}^{0.321}}\right) k_{\text{eq}}^{0.685 - 0.121 \log_{10}(\omega_{\text{b}})}.$$
 (1)

We also analyzed models with different primordial tilt  $n_{\rm s} \sim 2.5\sigma$  around the latest constraints [9], and found only a small dependence of  $k_{\rm max}$  on  $n_{\rm s}$ .

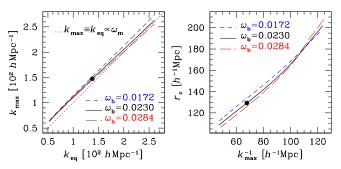


FIG. 2. P(k) turnover location  $k_{\text{max}}$  as a function of the horizon scale at matter-radiation equality  $k_{\text{eq}}$  (left panel), and its relation with the corresponding zero-crossing position  $r_{\text{c}}$  in the linear  $\xi(r)$  (right panel) for  $\Lambda\text{CDM}$  models with three different baryon densities. Solid symbols are for our fiducial model.

The existence of the turnover in the galaxy power spectrum has been discussed extensively in the literature, although its detection has not been reported up to now in any completed galaxy redshift survey such as the 2dF-GRS, SDSS or WiggleZ [5, 8, 12]. Yet, little attention has been paid to the imprint of the horizon scale at matterradiation equality on the zero-crossing in the galaxy twopoint correlation function  $\xi(r)$ . Although the very small clustering signal at those large scales is severely affected by potential sources of systematic errors [13, 14], here, in this letter, we highlight that the zero-crossing deserves momentous attention both from theory and observations. In the early 90s, Klypin & Rhee [15] proposed to use the zero-crossing measurements of the galaxy cluster CF as a sensitive test for the shape of the power spectrum of initial fluctuations. See also [16] for a detailed discussion on how, in their case, a sharp maximum in the power spectrum would be mapped into the correlation function.

The detection of the zero-crossing in  $\xi(r)$  is a fundamental prediction of  $\Lambda$ CDM or any other dark matter-baryon cosmological model [10, 17, 18]. The correlation function is related to P(k) by the Fourier transform [10]:

$$\xi(r) = \frac{1}{2\pi^2} \int_0^\infty dk k^2 P(k) \frac{\sin(kr)}{kr}.$$
 (2)

The correlation function must have a zero-crossing  $\xi(r_{\rm c})=0$  at some radius because  $P(k)\to 0$  when  $k\to 0$ , implying that  $\int_0^\infty \xi(r) r^2 dr=0$ . Note that for our fiducial model, the zero-crossing  $r_{\rm c}$  happens only at a scale  $\sim 20\%$  larger than the position of the BAO peak, i.e. at 129.3  $h^{-1}{\rm Mpc}$  (see Fig. 1, bottom panel).

However, the linear  $\xi(r)$  for models with  $\omega_{\rm m} \gtrsim 0.2$  shows a first zero-crossing located at scales  $r_{\rm c} \lesssim 80\,h^{-1}{\rm Mpc}$ , i.e. below the BAO feature (see Fig. 1). We recall that the SDSS and WiggleZ galaxy CFs display a positive clustering signal well above  $\sim 80\,h^{-1}{\rm Mpc}$ ,

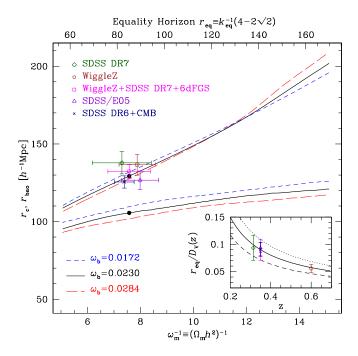


FIG. 3. Top curves show the zero-crossing scale  $r_c$  as a function of matter density  $\omega_m^{-1}$  and equality horizon size  $r_{\rm eq}$  (top axis) for our  $\Lambda$ CDM CAMB models with fixed values of  $\omega_b$ . This relation can be well represented by a broken power-law as given in Eq. (3). As a reference, we also show the acoustic peak position  $r_{\rm bao}$  (bottom curves). Solid symbol corresponds to our fiducial model. Zero-crossing estimates and 1- $\sigma$  errors obtained from best-fit  $\omega_m^{-1}$  and  $\alpha$  stretch parameters from different survey CF data are shown (open symbols). The inset panel shows the corresponding observational  $r_{\rm eq}/D_V(z)$  estimates for different redshifts. Also displayed are predictions for  $\Lambda$ CDM models with  $\omega_m=0.11$  (dashed line), 0.132 (fiducial, thick solid line) and 0.17 (dotted line).

at least up to the BAO peak located at  $\sim 105\,h^{-1}{\rm Mpc}$ , which already imposes a matter density upper limit of  $\omega_{\rm m} \sim 0.2$  (the stacked galaxy CF of these surveys gives a BAO detection at 4.9 $\sigma$  [19]). Here, we study the zero-crossing in  $\xi(r)$  located beyond the BAO feature for models with 50% matter density variation around our fiducial value, i.e.  $0.066 < \omega_{\rm m} < 0.198$ .

Fig. 2 (right panel) shows the relation between the zero-crossing position  $r_{\rm c}$  in the linear regime and its corresponding P(k) turnover location at  $k_{\rm max}$  for models with  $0.066 < \omega_{\rm m} < 0.198$ . It is clearly seen in Fig. 3 that  $r_{\rm c}$  is determined by the scale of the horizon at matter-radiation equality. Note, that  $r_{\rm c}$  shows a much steeper increase with  $\omega_{\rm m}^{-1}$  as compared with the position of the BAO peak  $r_{\rm bao}$ . Moreover, the BAO peak position shows a larger dependence on baryon density  $\omega_{\rm b}$ , e.g. about 7% and 3.5% variation in  $r_{\rm bao}$  and  $r_{\rm c}$  respectively at fiducial  $\omega_{\rm m}=0.132$  (solid point). The zero-crossing displays a small dependence on  $\omega_{\rm b}$  as can be seen in Eq. 1. For our grid of CAMB models with  $0.066 < \omega_{\rm m} < 0.198$  and  $0.0172 < \omega_{\rm b} < 0.0284$  we obtain the following relation

between the zero-crossing and the comoving size of the matter-radiation equality horizon, which is well described by a broken power-law, i.e.

$$r_{\rm c} = A r_{\rm eq}^{b_1} \left[ 1 + \left( \frac{r_{\rm eq}}{r_{\rm eq,0}} \right)^d \right]^{\frac{b_2 - b_1}{d}},$$
 (3)

where  $r_{\rm eq,0}=129.5\,h^{-1}{\rm Mpc}$ ,  $b_1=0.425$ , d=6.5. Parameters  $A=14.478\,\omega_b^{-0.0785}$ , and  $b_2=34.456\,\omega_b+0.171$  encode a slight dependence on baryon density. The size of the equality horizon  $r_{\rm eq}$  depends only on the equality characteristic scale  $k_{\rm eq}$  through the matter density, i.e.  $r_{\rm eq}\equiv (4-2\sqrt{2})\,k_{\rm eq}^{-1}=11.231\,\omega_{\rm m}^{-1}\,h^{-1}{\rm Mpc}$ .

To estimate the value of  $r_c$  with current galaxy surveys we use the constraints on the stretch parameter  $\alpha(z_{\text{eff}}) =$  $D_V(z_{\text{eff}})/D_{V,\text{fid}}(z_{\text{eff}}) \ (D_V(z) \equiv [(1+z)^2 D_A^2 cz/H(z)]^{1/3}$ is the dilation distance [4] and  $D_A$  is the angular diameter distance), obtained by different groups from their best-fit cosmology modeling to the observed SDSS and WiggleZ redshift-space  $\xi(s)$ . Typically, this model fit is done on the redshift-scale range  $20 h^{-1} \mathrm{Mpc} \lesssim s \lesssim$  $180 \,h^{-1}{\rm Mpc}$ . This allows us to estimate the expected position of the zero-crossing using the relation  $r_c$  =  $\alpha(z_{\rm eff}) r_{\rm c.fid}$ .  $D_{\rm V.fid}(z)$  and  $r_{\rm c.fid}$  are the dilation distance at  $z_{\rm eff}$  (survey mean redshift distribution) and the zerocrossing scale for the fiducial cosmology. Fig. 3 shows our estimates taking constraints on  $\alpha(z_{\text{eff}})$  and  $\omega_{\text{m}}$  from SDSS-LRG E05 [4], SDSS-LRG DR7 [19, 20], WiggleZ & Stacked WiggleZ+SDSS+6dFGS [19]; and SDSS-LRG DR6 combined with CMB [7].

The accurate modeling and interpretation of both P(k) and  $\xi(r)$  galaxy clustering statistics present some difficulties. The shape of the linear matter power spectrum P(k) is distorted by the nonlinear evolution of density fluctuations, redshift distortions and galaxy bias even at large-scales  $k < 0.2 \, h \mathrm{Mpc}^{-1}$  [21–24]. In this regard we should also draw attention to the impact of those inevitable effects on the expected zero-crossing scale in the redshift-space galaxy correlation function,  $\xi(s)$ , as imprinted by the horizon scale at matter-radiation equality.

We show in Fig. 4 redshift-space  $\xi(s)$  at z=0.5 (close to the mean redshift of the BOSS and WiggleZ galaxy distributions [8, 25]), drawn from our MultiDark and LittleMuk suite of N-body simulations of a flat  $\Lambda$ CDM cosmology with the same parameters as for our fiducial cosmological model. The MultiDark simulation (MDR1) was done using the ART code. It has 2048<sup>3</sup> particles in a  $1 h^{-1}$ Gpc box (see [26] and www.multidark.org for details). The mass and force resolutions are  $8.72 \times$  $10^9 \, h^{-1} \mathrm{M}_{\odot}$  and  $7 \, h^{-1} \mathrm{kpc}$ . LittleMuk (LMuk) consists of three GADGET [27] realizations of 1280<sup>3</sup> particles of a larger box with  $2.5 \,h^{-1}{\rm Gpc}$  on a side. Force resolution and particle mass are  $28 h^{-1}$ kpc and  $5.58 \times 10^{11} h^{-1}$ M<sub> $\odot$ </sub>. The LMuk total volume  $46.875 (h^{-1}\text{Gpc})^3$  allows us to compute the mean and the variance for the estimates of  $\xi(r)$  for dark matter halos. Dark matter halos (and subhalos) were identified with the Bound-Density-Maxima

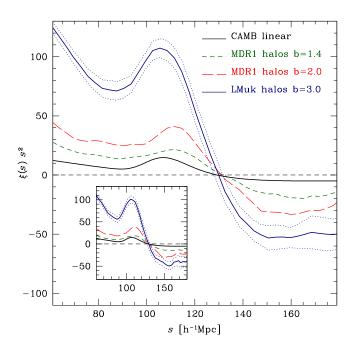


FIG. 4. Redshift-space correlation functions at z=0.5 for three halo ("galaxy") samples with different bias in the MultiDark and LittleMuk  $\Lambda$ CDM simulations. Results are compared with the linear  $\xi(r)$  (thick solid line) that corresponds to our fiducial cosmological parameters. The inset panel shows the real-space correlation function. The zero-crossing in real space is the same regardless of galaxy bias. There is a small  $\sim 0.4\%$  shift in the redshift-space. Dotted lines are statistical errors estimated for "galaxies" in the volume of  $46.875 \, (h^{-1}{\rm Gpc})^3$ .

(BDM) algorithm [26]. We then use a simple, non-parametric abundance-matching prescription, to connect dark matter halos (and subhalos) in our simulations with galaxies by selecting them above a given maximum circular velocity  $V_{\rm max}$ . This procedure is able to predict the clustering properties, and therefore the two-point CF and halo occupation distribution of observed galaxies for different number densities (e.g. [28, 29]).  $V_{\rm max}$  thresholds for the three "galaxy" samples with increasing biases indicated in the plot are 180, 350 and 600 km s<sup>-1</sup> roughly corresponding to the Emission Line Galaxies (ELGs, b=1.4), Luminous Red Galaxies (LRGs, b=2.0) and QSOs (b=3.0) in the major experiments discussed here.

Results presented in Fig. 4 evidence that the zero-crossing position  $r_{\rm c}$  in the dark matter halo CF appears at the location predicted by linear theory. Thus,  $r_{\rm c}$  is not distorted by the non-linear evolution of density fluctuations, redshift distortions and bias. This makes the zero-crossing an invaluable tool to constrain the size of the horizon at matter-radiation equality and the shape of the primordial power spectrum of initial fluctuations. We

measure  $r_c=129.8^{+7.2}_{-5.9}\,h^{-1}{\rm Mpc}$  from the mean LMuk "galaxy" sample (thin solid line in Fig. 4) with errors scaled according to statistics similar to that of the SDSS LRGs ( $\sim 10^5$  galaxies). Zero-crossing uncertainty goes down to a small value of  $\sim 1.5\%$  if we consider a survey with 10 times more galaxy statistics such as BOSS (dotted lines) or  $\sim 0.3\%$  in the case of 20 million galaxies, as it will be targeted by the upcoming new surveys like BigBOSS or Euclid. Our estimates are consistent with Fig. 6 in [30] for real- and redshift-space dark matter and halo samples of similar bias if one compares the expected zero-crossing  $r_{\rm c}$  position for their adopted cosmology. The level of systematics should be small enough to allow accurate measurements of  $r_{\rm c}$ . We estimate that the error in  $\xi(r)$  should be smaller than  $\sim 10^{-3}(3\times10^{-4})$ for 4(1)% error in  $r_{\rm c}$ .

Several groups have reported the absence of negative signal, and hence zero-crossing up to  $\sim 250\,h^{-1}{\rm Mpc}$  (see [20, 31] and references therein). It was speculated in [32] that the large-scale SDSS  $\xi(s)$  is affected by intrinsic errors and volume-dependent systematic effects. The implications of a possible constant systematic shift in the redshift-space clustering due to unknown observational systematic errors has been pointed out in [7]. It was argued in [20] that lack of zero crossing in SDSS was simply due to cosmic variance, not unknown systematics. Interestingly, the WiggleZ redshift-space  $\xi(s)$  at z=0.6 [8], albeit with large uncertainties, displays a crossover around  $\sim 120\,h^{-1}{\rm Mpc}$  and negative signal above this scale up to  $180\,h^{-1}{\rm Mpc}$ , as expected for current matter density observational constraints.

We believe that the detection of the zero-crossing in the galaxy correlation function may offer some advantages as compared with finding the maximum in P(k), though mathematically both are equivalent. The individual Fourier modes in P(k) split the clustering signal in fragments and as a result the signal-to-noise and accuracy are expected to be smaller as compared with the cross-correlation signal around the zero-crossing which is coming from the convolution of the entire P(k) without any binning or splitting of the signal.

To summarize, adding zero-crossing estimates will improve the accuracy of  $\omega_{\rm m}$  because  $r_{\rm c}$  is more sensitive to  $\omega_{\rm m}$  than the BAO peak and because it does not require the elaborate reconstruction methods used for BAO analysis [33, 34].

We thank A. Kravtsov, C. Blake, A. Sanchez, and D. Eisenstein for fruitful discussions and comments. We are grateful to S. Knollmann for running LMuk initial conditions. MDR1 and LMuk simulations were run on NASA's Pleiades and SuperMUC Migration system at LRZ München. This work is supported by Spanish (AYA10-21231, Multidark-CSD2009-0064, SyeC-CSD2007-0050, AYA09-13875), German (DAAD, DFG-MU1020-16-1) and US NSF grants to NMSU.

- [1] J. A. Frieman and et al., ARAA 46, 385 (2008).
- [2] D. J. Eisenstein and W. Hu, ApJ 496, 605 (1998).
- [3] D. J. Eisenstein and W. Hu, ApJ **511**, 5 (1999).
- [4] D. J. Eisenstein and et al., ApJ **633**, 560 (2005).
- [5] S. Cole and et al., MNRAS **362**, 505 (2005).
- [6] W. J. Percival and et al., MNRAS 401, 2148 (2010).
- [7] A. G. Sánchez and et al., MNRAS 400, 1643 (2009).
- [8] C. Blake and et al., MNRAS **415**, 2892 (2011).
- [9] E. Komatsu and et al., ApJS **192**, 18 (2011).
- [10] P. J. E. Peebles, The large-scale structure of the universe, Princeton University Press (1980).
- [11] A. Lewis and et al., ApJ **538**, 473 (2000).
- [12] B. A. Reid and et al., MNRAS 404, 60 (2010).
- [13] C. Blake and S. Bridle, MNRAS **363**, 1329 (2005).
- [14] A. J. Ross and et al., MNRAS, 1393 (2011).
- [15] A. Klypin and G. Rhee, ApJ **428**, 399 (1994).
- [16] J. Einasto and et al., MNRAS 289, 813 (1997).

- [17] A. Gabrielli and et al., PRD **65**, 083523 (2002).
- [18] T. Matsubara, ApJ **615**, 573 (2004).
- [19] C. Blake and et al., (2011), arXiv:1108.2635.
- [20] E. A. Kazin and et al., ApJ **710**, 1444 (2010).
- [21] R. E. Smith and et al., MNRAS **341**, 1311 (2003).
- [22] M. Crocce and R. Scoccimarro, PRD 73, 063519 (2006).
- [23] H.-J. Seo and et al., ApJ **686**, 13 (2008).
- [24] R. E. Angulo and et al., MNRAS 383, 755 (2008).
- [25] M. White and et al., ApJ 728, 126 (2011).
- [26] F. Prada and et al., (2011), arXiv:1104.5130.
- [27] V. Springel, MNRAS **364**, 1105 (2005).
- [28] C. Conroy and et al., ApJ 647, 201 (2006).
- [29] S. Trujillo-Gomez and et al., (2010), arXiv:1005.1289.
- [30] A. G. Sánchez and et al., MNRAS 390, 1470 (2008).
- [31] V. J. Martínez and et al., ApJL 696, L93 (2009).
- [32] F. Sylos Labini and et al., AA **505**, 981 (2009).
- [33] D. J. Eisenstein and et al., ApJ **664**, 675 (2007).
- [34] N. Padmanabhan and et al., PRD 79, 063523 (2009).